Available online at www.sciencedirect.com
SCIENCE DIRECT®
Developmental Biology 288 (2005) 179 – 193
DEVELOPMENTAL BIOLOGY
www.elsevier.com/locate/ydbio

mummy/cystic encodes an enzyme required for chitin and glycan synthesis, involved in trachea, embryonic cuticle and CNS development—Analysis of its role in *Drosophila* tracheal morphogenesis

Sofia J. Araújo [a,1], Hanna Aslam [b,1], Guy Tear [b], Jordi Casanova [a,*]

[a] *Institut de Biologia Molecular de Barcelona (CSIC), Parc Cientific de Barcelona, Carrer Josep Samitier 1-5, 08028 Barcelona, Spain*
[b] *MRC Centre for Developmental Neurobiology, New Hunt's House, Guy's Hospital Campus, London SE1 1UL, UK*

Received for publication 18 July 2005, revised 9 September 2005, accepted 11 September 2005
Available online 8 November 2005

Abstract

Tracheal and nervous system development are two model systems for the study of organogenesis in *Drosophila*. In two independent screens, we identified three alleles of a gene involved in tracheal, cuticle and CNS development. Here, we show that these alleles, and the previously identified *cystic* and *mummy*, all belong to the same complementation group. These are mutants of a gene encoding the UDP-*N*-acetylglucosamine diphosphorylase, an enzyme responsible for the production of UDP-*N*-acetylglucosamine, an important intermediate in chitin and glycan biosynthesis. *cyst* was originally singled out as a gene required for the regulation of tracheal tube diameter. We characterized the *cyst*/*mmy* tracheal phenotype and upon histological examination concluded that *mmy* mutant embryos lack chitin-containing structures, such as the procuticle at the epidermis and the taenidial folds in the tracheal lumen. While most of their tracheal morphogenesis defects can be attributed to the lack of chitin, when compared to *krotzkopf verkehrt* (*kkv*) chitin-synthase mutants, *mmy* mutants showed a stronger phenotype, suggesting that some of the *mmy* phenotypes, like the axon guidance defects, are chitin-independent. We discuss the implications of these new data in the mechanism of size control in the *Drosophila* trachea.

Keywords: *mmy*; *cyst*; *kkv*; Chitin; UDP-*N*-acetylglucosamine diphosphorylase; GlcNAc; Tracheal system; CNS; Cuticle; *Drosophila*; Morphogenesis

Introduction

Organogenesis is a complex developmental process that involves changes in cell populations in terms of their proliferation, migration, differentiation and shape. These events must be coordinated in order to generate organs whose component parts are integrated into a functional unit that reaches and maintains a particular final size.

Several model systems have emerged for the study of organogenesis. Namely, the nervous and tracheal systems have helped us understand many of the mechanisms and molecular pathways involved in organ formation. The *Drosophila* tracheal system has proven to be a particularly appropriate model for the study of tubulogenesis. The larval tracheal system of *Drosophila* is a complex tubular network that conducts oxygen from the exterior to the internal tissues. It arises from the tracheal placodes, clusters of ectodermal cells that appear at each side of 10 embryonic segments, from the 2nd thoracic segment to the 8th abdominal segment. The cells of each cluster invaginate and migrate in a stereotypic pattern to form each of the primary tracheal branches (reviewed in Manning and Krasnow, 1993). The general conclusion from many studies is that the direction of migration of the tracheal cells relies on a set of positional cues provided by nearby cells (Sutherland et al., 1996; Llimargas, 2000; Llimargas and Casanova, 1997; Vincent et al., 1997; Wappner et al., 1997; Chihara and Hayashi, 2000). In addition, the establishment of interactions between tracheal cells and their substrates is a crucial step in tracheal cell migration, a process ultimately determined by molecules expressed at their surface (Franch-Marro and Casanova, 2000; Boube et al., 2001).

Genetic analyses have identified many genes required for specific steps of tracheal morphogenesis, such as tube fusion and cell intercalation during formation of finer branches

* Corresponding author. Fax: +34934034979.
E-mail address: jcrbmc@cid.csic.es (J. Casanova).
[1] Joint first authors.

0012-1606/$ - see front matter © 2005 Elsevier Inc. All rights reserved.
doi:10.1016/j.ydbio.2005.09.031

(Samakovlis et al., 1996b; Tanaka-Matakatsu et al., 1996; Ikeya and Hayashi, 1999; Llimargas, 1999; Steneberg et al., 1999; Lee and Kolodziej, 2002; Jazwinska et al., 2003; Ribeiro et al., 2004). One of the features of the tracheal system is that the tubes in each branch have specific sizes and diameters that appear to be precisely regulated during development (Beitel and Krasnow, 2000). Several genes have been reported to affect the size of the tracheal tubes. Among these, a group of genes originally identified as controlling tube length have been found to code for proteins belonging to or associated with the septate junctions (SJs) (Behr et al., 2003; Hemphala et al., 2003; Paul et al., 2003; Llimargas et al., 2004; Wu et al., 2004). Another gene, *cystic* (*cyst*), was previously singled out as being specifically required for the regulation of tracheal tube diameter (Beitel and Krasnow, 2000). Here, we report the identification of further alleles of *cystic*; that *cyst* is allelic to the previously identified *mummy* (*mmy*) gene (Nüsslein-Volhard et al., 1984); that *cyst/mmy* is required for cuticle formation and the morphogenesis of the central nervous system (CNS); and that it encodes the only predicted *Drosophila melanogaster* UDP-*N*-acetylglucosamine diphosphorylase (UDP-GlcNAc diphosphorylase; also named UDP-*N*-acetylglucosamine pyrophosphorylase). This enzyme is required for the synthesis of UDP-*N*-acetylglucosamine (UDP-GlcNAc), a substrate for chitin and glycan synthesis (Herscovics and Orlean, 1993; Merzendorfer and Zimoch, 2003). Accordingly, we show that *cyst/mmy* is required for chitin deposition in the trachea and for the formation of the embryonic cuticle. Finally, we describe the tracheal defects associated with the *cyst/mmy* mutant phenotype and discuss the implications on the mechanism of tracheal tube size control.

Results

mummy, cystic and a set of newly induced mutations define a single complementation group required for trachea morphogenesis, CNS development and cuticle formation

To identify new genes involved in tracheal morphogenesis, we screened a collection of EMS-induced mutants using the 2A12 antiserum that recognizes an epitope at the lumen of the tracheal tubes. Among the new mutants found, one (H053) did not display a continuous luminal structure and instead showed a very dispersed tracheal staining (Figs. 1C, D). Upon examination of these mutant embryos with an antibody recognizing the *trachealess* (*trh*) gene product, we confirmed that the tracheal cells in these embryos were present and were reasonably positioned in a tubular manner similar to the wild-type (Figs. 1E, F). However, after more detailed analysis, we could detect that the arrangement of the cells in H053 was rather distorted, lacking their typical aligned structure (Figs. 1G, H).

In an independent screen for mutants showing CNS phenotypes, we identified two mutants (GA74 and GA760) with a subtle CNS phenotype where the commissural pathways appear diffuse and there is a reduction in the thickness of the longitudinal tracts (Fig. 2B). The fasciclin-II-positive fascicles within these embryos are not as well defined as in wild-type, and fasciclin-II-positive axons are observed extending towards the midline (Fig. 2D). These phenotypes are characteristic of defects in midline signaling (reviewed in Araújo and Tear, 2003).

Further examination of the mutant phenotypes showed that both H053 and GA74 mutants displayed simultaneously the tracheal and CNS phenotype. Both mutants were uncovered by the same deficiencies (see below), and a complementation analysis showed that they failed to complement one another, both for lethality and the embryonic phenotypes. Therefore, H053 and GA74 define a single complementation group. During the phenotypic analysis of these mutants, we realized that their tracheal defect is reminiscent of that previously described for the *cystic* (*cyst*) mutant (Beitel and Krasnow, 2000). We also observed that H053, GA74 and *cyst* display a cuticle phenotype similar to that seen in *mummy* (*mmy*) mutants (Nüsslein-Volhard et al., 1984). In addition, we found that the *cyst* and *mmy* mutations were also uncovered by the same deficiencies (see below), and all these independently induced mutants failed to complement each other; therefore, they are alleles of the same gene. As *mummy* (*mmy*) is the name of the earliest induced mutant, we have retained this name for all the alleles.

mummy encodes an UDP-N-acetylglucosamine diphosphorylase

To identify the genomic location of the *mmy* gene affected in the tracheal and CNS mutants, two alleles, mmy^{GA74} and mmy^{GA760}, were mapped by performing a lethal complementation analysis with a set of deficiencies from the Bloomington Stock Center. This revealed that Df(2L)BSC6, which deletes the region 26D3-E1 to 26F4-7, fails to complement the *mmy* alleles. An overlapping deficiency from the DrosDel collection that removes 26C1 to 26D7, Df(2L)ED380, complemented the alleles as did a neighboring Bloomington deficiency, Df(2L)BSC7, that deletes the interval from 26D10-E1 to 27C1. This revealed that the *mmy* gene lies in the region 26D7-26E1 (Fig. 3A). A series of lethal P-element insertions in this region were tested, and the insertion KG08617 failed to complement all *mmy* alleles. Transheterozygote combinations of mmy^{GA74} with KG08617 displayed the same phenotypes as the mmy^{GA74} homozygotes, suggesting that the gene disrupted by KG08617 is *mmy*. KG08617 is inserted within an intron of the predicted gene CG9535, suggesting that CG9535 is the gene responsible for the *mmy* phenotype. To confirm this, the P-element was excised precisely which resulted in reversion to wild-type. To further confirm that CG9535 is affected in the mutants, the mmy^{GA74} and mmy^{H053} chromosomes were sequenced to reveal changes of Val419Asp and Trp199STOP, respectively (Fig. 3B).

CG9535/*mmy* encodes a protein with significant homology to the UDP-*N*-acetylglucosamine pyrophosphorylases. This enzyme catalyzes the formation of UDP-*N*-acetylglucosamine (UDP-GlcNAc), the activated form of *N*-acetylglucosamine

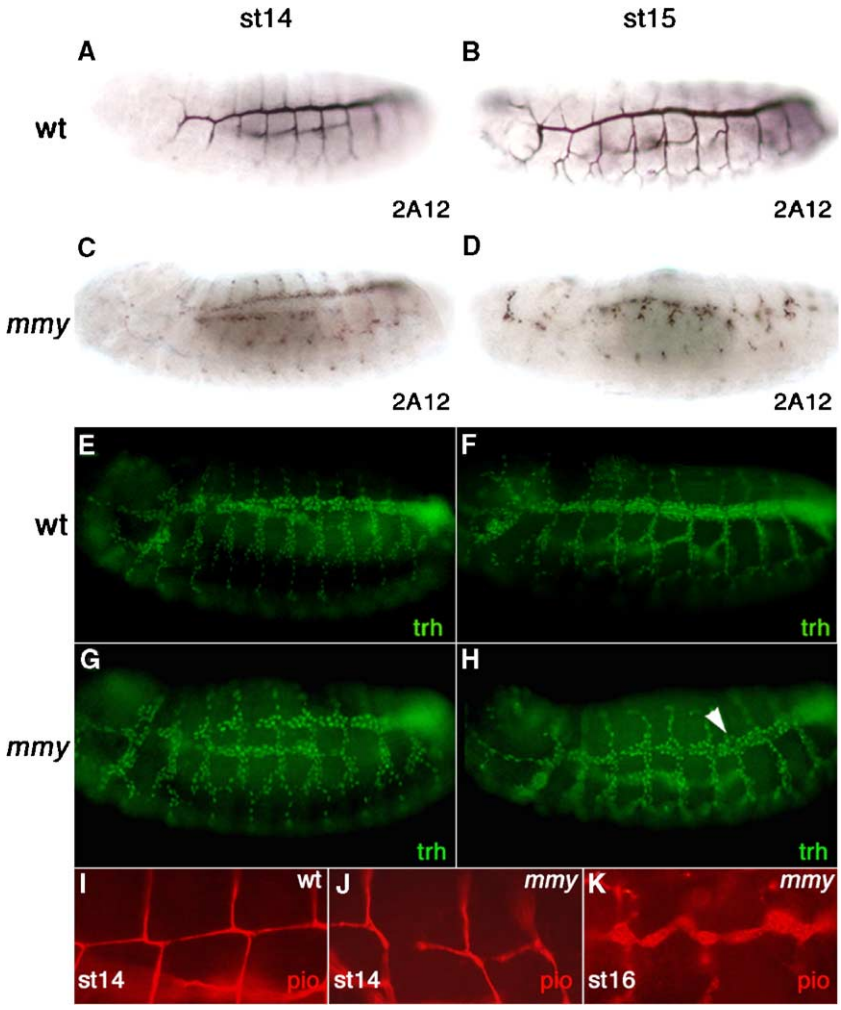

Fig. 1. *mummy* mutants have tracheal defects. All *mmy* alleles display a strong phenotype in the tracheal system. Detection of 2A12 tracheal lumen antigen during stages 14 and 15 in wild-type (A, B) and mmy^{H053} mutant embryos (C, D), showing the discontinuous appearance of the tracheal lumen characteristic of *mmy* mutants. Trachealess protein in stages 14 and 15 mmy^{H053} embryos (G, H) showing correct migration of the tracheal cells but general disorganization in comparison with wild-type (E, F). At stage 15, some of the tracheal cells in *mmy* are already found in bubble-like structures (arrowhead in panel H). Our trachealess antibody detects the nuclei of the tracheal cells where Trachealess protein localizes but additionally detects a luminal epitope at later stages (15–16). Detection of Piopio luminal protein in stage 14 wild-type (I) and stages 14 and 16 mmy^{H053} mutant embryos (J, K). Anterior is left and dorsal is up in all pictures.

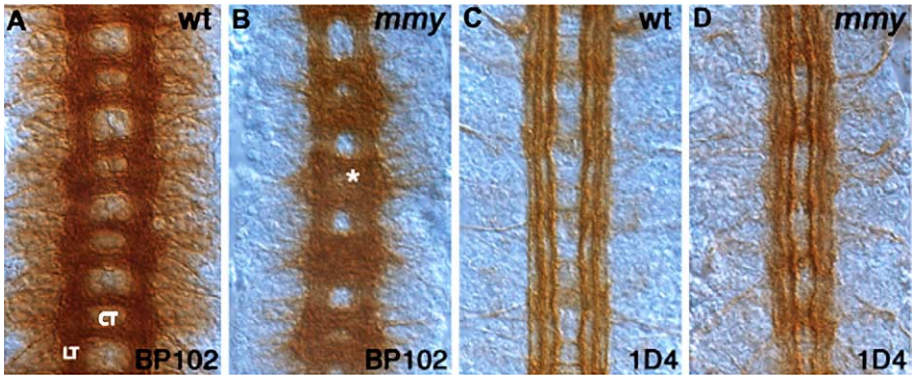

Fig. 2. *mummy* is required for the normal development of the central nervous system. All *mummy* alleles display a phenotype in the central nervous system as revealed using Mab BP102 (A and B) and 1D4, anti-fasciclin-II (C and D). (A) In the stage 15 wild-type embryo, the CNS axon tracts are organized into a characteristic orthogonal structure of longitudinal tracts (LT) connected in each segment by a pair of commissural tracts (CT). (B) In mmy^{KG8617}, as in all alleles, the commissural tracts are not separated correctly and can become fused (asterisk), while the longitudinal tracts are diminished. (C) In the stage 16 wild-type embryo, three clear longitudinal fascicles are revealed by anti-fasciclin-II. (D) In mmy^{GA74}, as in all alleles, these tracts are less distinct and are positioned closer to the midline. Anterior is up in all panels.

(GlcNAc), which is a key precursor necessary for N- and O-linked glycosylation of proteins (Mio et al., 1998; Peneff et al., 2001; Bulik et al., 2000). It is the major substrate for the synthesis of chitin and is also essential for the formation of the glycosylphosphatidylinositol (GPI) linker that anchors many cell surface molecules to the plasma membrane (Fig. 3B′).

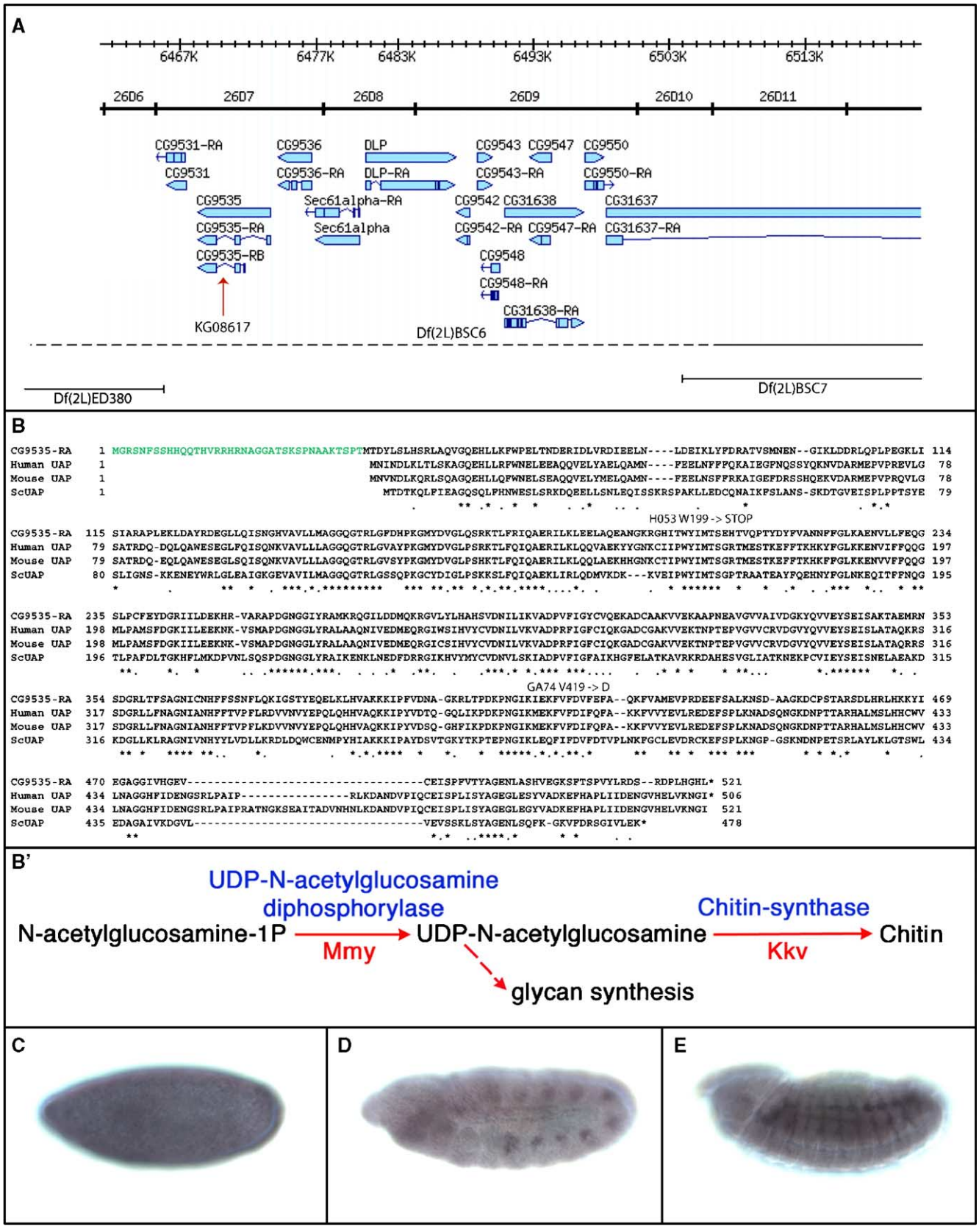

Reduction in the activity of this enzyme is therefore anticipated to affect a number of downstream pathways.

Two alternative transcripts have been identified for the gene that differ in their use of first exon (Fig. 3A). These encode two proteins of 520 and 483 amino acids, the larger protein contains an additional 37 amino acids at its N-terminal and shares the same 483 amino acids of the smaller protein (http://www.flybase.bio.indiana.edu). Each of the sequenced alleles affects both proteins. In *mmy*^{GA74}, a valine at position 499 (in the larger protein) is predicted to be replaced by an aspartic acid. As this residue lies between two conserved phenylalanines that both bind the nucleotide-sugar, it is likely that this change affects substrate binding (Peneff et al., 2001). In *mmy*^{H053}, a premature stop codon is created at position 199 to truncate both proteins (Fig. 3B).

We examined the expression of this gene using a probe that detects both transcripts. This revealed that the gene is maternally loaded as high levels of transcript are seen in freshly laid eggs (Fig. 3C). This ubiquitous expression declines and is reduced to a low level by stage 6. Subsequent to this, a high level of transcription occurs in the developing trachea. Expression is noticeable from stage 11 when the tracheal placodes form (Fig. 3D). This level of expression is maintained in the trachea as their development proceeds, with expression continuing throughout all tracheal branches until stage 16. In mature embryos, we also detected expression throughout the epidermis.

The mmy tracheal phenotype

Tracheal development begins normally in *mmy* mutant embryos as monitored by the anti-Trh antibody. Placodes are correctly positioned, and migration occurs normally in different directions to form the distinct tracheal branches (data not shown). Thus, the initial steps of tracheal development are apparently normal until the event of tube formation. From late stage 14, we detected that the pattern of tracheal cells was not as well organized as in the wild-type. In particular, tracheal nuclei were no longer regularly spaced and did not form linear rows in the dorsal trunk (Figs. 1G, H). These defects worsen as development proceeds; by stage 16, the tracheal nuclei outlined an irregular dorsal trunk of variable width leading to the formation of a tube with constrictions, breaks and dilations along its entire length. We also analyzed the tracheal cell shape during development by detecting a UAStauGFP construct under a breathless-GAL4 promoter, a specific driver for all tracheal cells. Again, cells appeared to behave normally until the stage of tube formation when they adopted an irregular organization forming tubular structures of bubble-like appearance (Figs. 4J–L).

The original analysis of the *mmy* tracheal phenotype using the 2A12 antibody showed a discontinuous lumenal structure (Figs. 1C, D). To further investigate this, we analyzed the localization of the Piopio protein. In wild-type embryos, Pio accumulates in the tracheal lumen where it is thought to be part of the extracellular matrix that provides a structural network in the luminal space (Jazwinska et al., 2003). Pio accumulation appeared normal in the *mmy* trachea, but, at stage 14, when wild-type embryos already showed a continuous lumen, the *mmy* lumen displayed interruptions between metameres, suggesting a lack of a continuous luminal structure or a delay in the fusion process (Figs. 1G, H). Noticeably, the general accumulation of Pio seemed to be unaffected in *mmy* mutants, as opposed to the accumulation of the lumen epitope recognized by the 2A12 antibody, suggesting that different luminal structures present in the tracheal tubes have different requirements for localization. At stage 16, Pio accumulation was still lumenal, highlighting the bubble-like appearance of the dorsal trunk (Fig. 1I).

How can a UDP-GlcNAc diphosphorylase affect tracheal morphogenesis? This enzyme plays a key role in the metabolic pathway leading to chitin formation, a component of the tracheal cuticle and a main component of the arthropod exoskeleton. UDP-GlcNAc is the major constituent of chitin and the substrate for chitin synthase (Merzendorfer and Zimoch, 2003). In the embryo, chitin can be visualized by the incorporation of Fluostain (Moussian et al., 2005), and terminal GlcNAc residues can be detected by wheat germ agglutinin (WGA), a lectin (Wright, 1984).

We stained *mmy* embryos with Fluostain and found that chitin was not present in the trachea of these mutants, suggesting that this could be the cause of their tracheal phenotype (Figs. 4A, B). In addition, WGA incorporation in *mmy* embryos was practically absent, revealing the lack of terminal GlcNAc residues at the cell surface. In wild-type embryos, WGA stained both apical and basal cell surfaces and accumulated in the tracheal lumen, cuticle and gut (Figs. 4A, H). In mature *mmy* embryos, however, we could detect only a very faint staining at the surface of cells (Fig. 4K).

Fig. 3. Identification of the *mummy* gene. (A) Genomic region that contains the *mummy* gene. Lower section shows the extent of deficiencies used in the mapping of mummy. Df(2L)BSC6 is deficient for the region (the dotted line indicates uncertainty on the precise endpoint of the deficiency). The regions removed by the deficiencies Df(2L)BSC7 and Df(2L)ED380 are indicated by the continuous lines. In the upper panel, the location of the P-element KG08617 that disrupts *mummy* is illustrated. (B) The proteins encoded by *mummy*/CG9535 show considerable homology to UDP-*N*-acetylglucosamine diphosphorylases (UAPs) from human to yeast (ScUAP). *mummy* encodes two transcripts the longer of which encodes a protein that has an additional 37 amino acids at the N-terminus (shown in green). Two *mummy* alleles affect regions common to both isoforms. The position of the EMS-induced mutations is indicated in the protein sequence, H053 introduces a stop codon at 199, while GA74 introduces a non-conservative amino acid change Val to Asp at 419. (B′) Schematic representation of the reaction catalyzed by UDP-*N*-acetylglucosamine diphosphorylase generating UDP-GlcNAc. This is followed by the polymerization reaction catalyzed by CS-1/Kkv to produce chitin (adapted from Merzendorfer and Zimoch, 2003). (C–E) Expression of the *mummy* gene as revealed by a probe that detects both transcripts. (C) *mummy* transcript is loaded into the egg by the mother. (D) High levels of zygotic expression are detected at stage 11 in the tracheal placodes, this high level of expression continues in the trachea as they develop their branches in stage 15 (E) and continues until stage 17, where it is also detected at the epidermis/cuticle. Expression in the salivary glands and gut is detected throughout the development of these organs (D, E and data not shown). Low level expression of *mummy* is also visible in all cells.

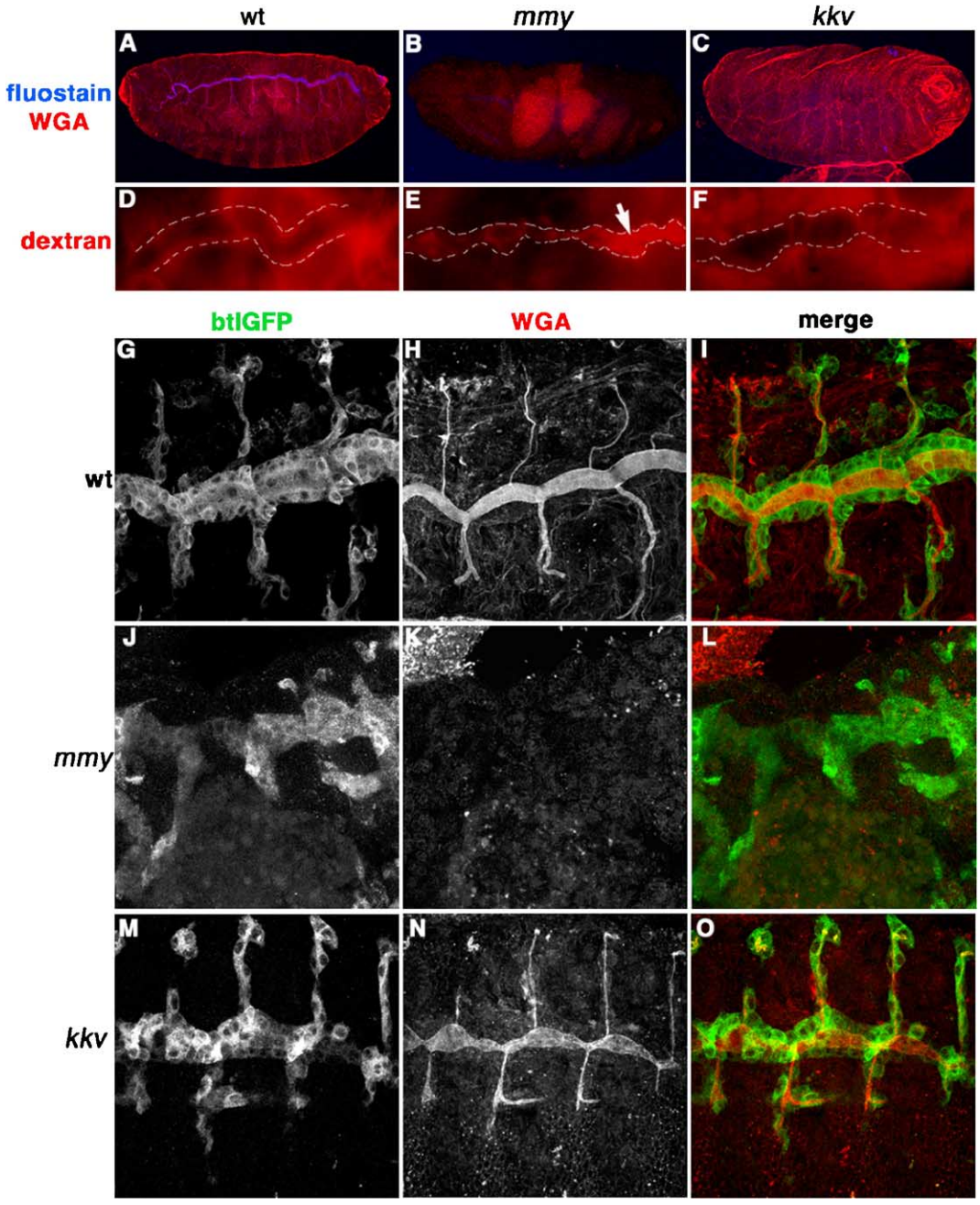

Fig. 4. *mummy* mutants do not synthesize chitin. (A, B and C) Presence of chitin and terminal *N*-acetylglucosamine residues in wild-type, *mmy* and *kkv* stage 16 embryos. Chitin (blue) is detected in wild-type (A) but not in *mmy* (B) or *kkv* mutants (C). *N*-acetylglucosamine (red) is strongly detected in the trachea and epidermis of wild-type (A) and *kkv* mutants (C), but not in *mmy* mutants (despite some background accumulation of fluorescence in the gut). (D, E and F) The integrity of the septate junction diffusion barrier was tested by a dye permeability assay. Wild-type and *kkv* trachea are not permeable to fluorescently labeled 10 kDa dextran dye injected into the body cavity (D and F). *mmy* trachea is permeable to the dye in some stretches of the dorsal trunk (arrow in panel E) but not in others, showing that the lack of permeability is not attributable to a general problem of all cells in the dorsal trunk. The tracheal cell contour is highlighted by a dashed white line. (G–O) Confocal projections of wild-type (G–I), *mmy* (J–L) and *kkv* (M–O) stage 16 embryos stained with anti-GFP (in green) to detect the expression of tauGFP construct that marks the tracheal cell shape and WGA (red) to detect *N*-acetylglucosamine residues in the tracheal lumen. Anterior is left, and dorsal is up (except in panels D–E that are dorsal views of injected mature embryos).

Previous reports indicated that the tracheal epithelium of mmy^{cyst} mutants is permeable as assessed by a dye permeability assay, suggesting a loss of the trans-epithelial diffusion barrier in this mutant (Paul et al., 2003). This is a relevant point since septate junctions (SJs), which have a prominent role in the establishment of this diffusion barrier, have also been shown to be critical for the control of tracheal tube size (Wu and Beitel, 2004). For this reason, we tested whether SJs could be affected in *mmy* mutants. Contrary to what we observed in mutants for SJ components (data not shown), we found that upon dye injection the diffusion barrier was not completely abolished in the *mmy* trachea. Rather, some independent tracks of the tube remained impermeable, while others showed a loss of the diffusion barrier as judged by dye uptake (Figs. 4D, E).

These results suggested that the general diffusion barrier mechanism mediated by the SJs was not wholly impaired in *mmy* mutants. On the contrary, breaks and discontinuities within the lumen of the tube could be the origin of the permeabilization defects.

Supporting the permeabilization results, we observed that, even at late embryonic stages, when the tube is severely affected, components of the SJs such as Coracle (Cora) (Fehon et al., 1994) and Discs-large (Dlg) (Woods and Bryant, 1991) maintained a correct localization both in the tracheal tubes, epidermis and salivary glands (Figs. 5E–P). In addition, Stranded-at-second (Sas), a marker for the apical surface of cells (Schonbaum et al., 1992), showed a correct localization in *mmy* (Figs. 5A–D). Taken together, these results indicate that the apical/basal polarity of the mutant cells is maintained and that the SJ components are not mislocalized in *mmy* embryos.

By marking the cytoplasm of the tracheal cells with GFP, we detected that, despite the bubble-like appearance of the dorsal trunk, its cells still displayed structural continuity. But, even though there was a continuity between the cells of the dorsal trunk, its lumen formed separate bubble-like structures (Figs. 5A–D). The peculiar morphology of the *mmy* mutant trachea suggested to us that the observed phenotype could be due to incorrect lumenal fusion and expansion between the independent tubular structures from adjacent metameres. An important step in this process is the formation of three cadherin rings at the fusion point. Complete failure of fusion, due to mutations in E-cadherin, leads to the formation of separate unfused structures in each metamere (Tanaka-Matakatsu et al., 1996). In spite of detecting the presence of E-cadherin on the surface of cells in *mmy* embryos, we were not able to observe the formation of the cadherin rings in their dorsal trunk, suggesting that the correct fusion of the two adjacent lumens into a continuous tube was not fully achieved (Figs. 5Q–T). These cadherin rings are the result of the fusion process and, at late embryonic stages, mark the site where the lumen connections occur after fusion of the dorsal trunk cells. In order to check for the presence of fusion cells in *mmy* embryos, we analyzed the expression of two markers that are characteristic of these cell types, Fusion-3 and Headcase. Fusion-3 is expressed in all fusion cells from stage 13/14, and Headcase is expressed in all but the dorsal trunk fusion cells from stage 15 (Samakovlis et al., 1996a; Steneberg et al., 1998). Both markers were detected in *mmy* as in the wild-type (Figs. 5U–X and data not shown), indicating that fusion cells appear to be correctly specified in *mmy* mutants, although fusion is not completely accomplished.

All the above results suggested that the absence of chitin could be the main cause of the abnormal shape of the *mmy* tracheal system. To corroborate this hypothesis and to examine tube architecture in *mmy* embryos, we performed transmission electron microscopy (TEM) analysis of the tracheal system of mature *mmy* embryos (Fig. 6). Three main features were recognized at the ultrastructural level that diverged from the wild-type organization of the tracheal lumen. First, the taenidial folds inside the tubes were not properly formed (Fig. 6, compare A and B). The taenidial folds are annular rings around the tracheal lumen that are thought to be important to give some stiffness to the tubes and to allow them to expand and contract along their length (reviewed in Manning and Krasnow, 1993). These taenidia, which become visible as cuticular protrusions in transverse and longitudinal sections, were not present in the tracheal lumen of *mmy* embryos (Figs. 6B and E–G). Second, in contrast to what occurs in the wild-type, the luminal structures were not in close apposition to the membranes of the surrounding tracheal cells; instead, the lining of the tube appeared detached (Fig. 6, asterisks). Third, in *mmy* embryos, at the apical membranes of the tracheal cells, we detected a higher number of microvillae than in same stage wild-type embryos. Microvillae are detected during the first steps of envelope formation and are thought to have an active role in the formation of cuticular structures (Locke, 2001). In *mmy* mutants, perhaps due to incorrect synthesis of cuticular luminal components, these microvillae continued to be detected at later stages than in wild-type embryos. As a consequence, the apical side of the epidermal cells does not form a continuous structure with the lumen.

Taken together, these observations lead to the conclusion that the tracheal lumen of *mmy* embryos is missing the characteristic luminal architecture present in the wild-type trachea and that this can be related to the lack of the cuticular structures due to chitin absence.

Comparison of the mmy mutant phenotype with a mutant for the chitin synthase

To assess the requirement of chitin in the proper organization of the tracheal system, we analyzed whether similar mutant phenotypes were found in other mutants that affect chitin synthesis. Recently, it has been shown that the *krotzkopf verkehrt* (*kkv*) gene encodes a chitin synthase enzyme (CS-1); as a result, there is no chitin in the trachea of *kkv* embryos (Ostrowski et al., 2002; Moussian et al., 2005). Since both the Mmy and Kkv enzymes are involved in the later stages of the chitin synthesis pathway (Fig. 3), we extended the analysis of the *kkv* mutant trachea and compared it to *mmy*.

We found that *kkv* tracheal tubes were similar to the tubes in *mmy* mutant embryos as they displayed comparable constrictions and dilations. However, the overall tube structure in *kkv* was not as distorted (Fig. 4, compare L to O). Specifically, the dorsal trunk lumen of *kkv* mutants was continuous (Figs. 4M–O) and did not show the fragmented and separated bubble-like structures present in the *mmy* mutants (Figs. 5C, D). This correlates with the observation that the cadherin rings produced by the fusion cells were present in the *kkv* mutant dorsal trunk, suggesting that the fusion process has allowed the formation of a continuous dorsal trunk lumen (data not shown). We also performed a dye permeability assay to test the trans-epithelial diffusion barrier in *kkv* mutants. As in wild-type, the rhodamine-labeled dextran did not show any diffusion into the tracheal lumen (Fig. 4F), indicating that the diffusion barrier mechanism mediated by the SJs is not impaired in *kkv* mutants.

In addition, we could not detect any CNS phenotypes in *kkv* embryos (data not shown). The CNS of *kkv* mutants is

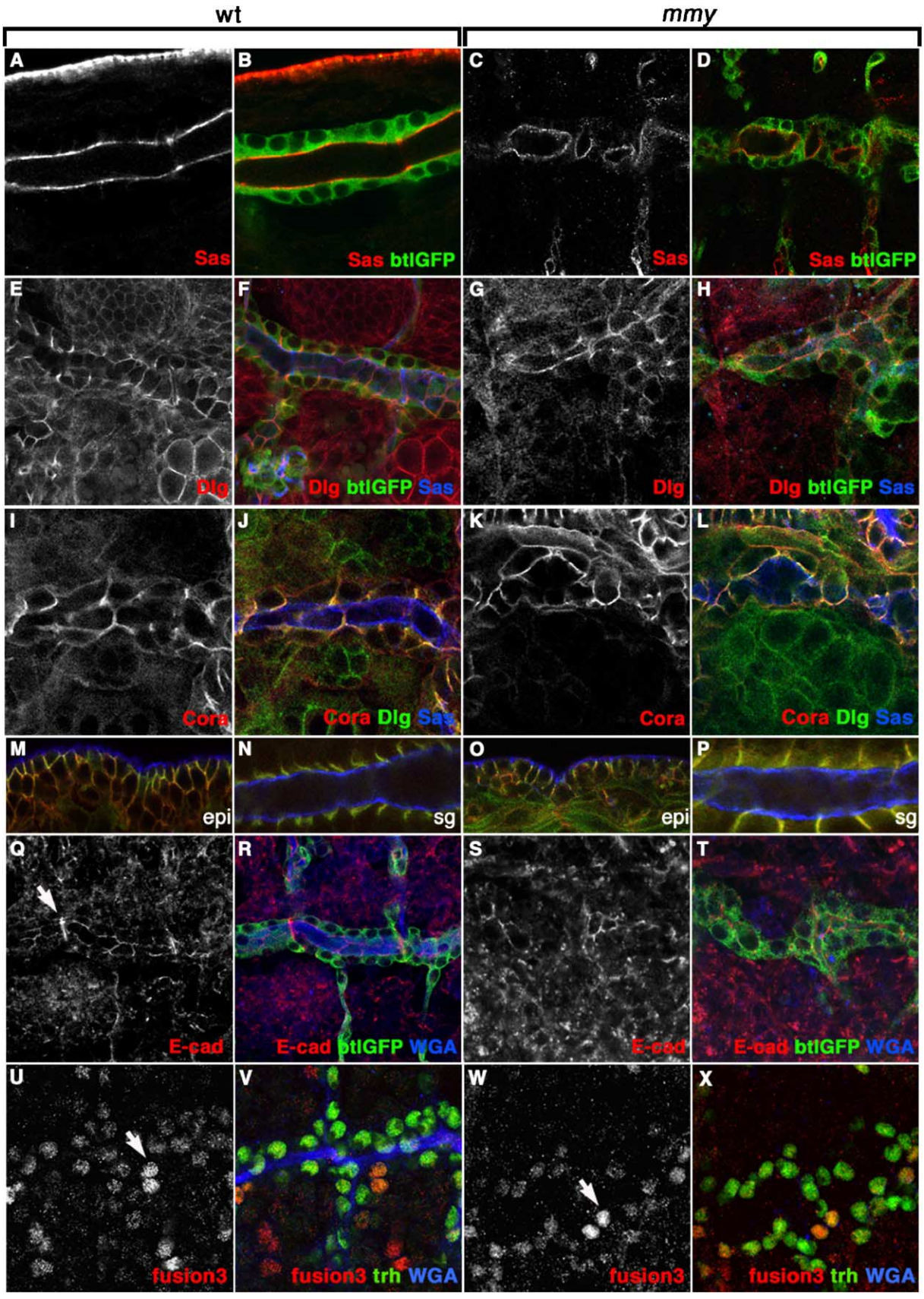
wt
mmy
A
Sas
B
Sas btlGFP
C
Sas
D
Sas btlGFP
E
Dlg
F
Dlg btlGFP Sas
G
Dlg
H
Dlg btlGFP Sas
I
Cora
J
Cora Dlg Sas
K
Cora
L
Cora Dlg Sas
M
epi
N
sg
O
epi
P
sg
Q
E-cad
R
E-cad btlGFP WGA
S
E-cad
T
E-cad btlGFP WGA
U
fusion3
V
fusion3 trh WGA
W
fusion3
X
fusion3 trh WGA

apparently normal, which supports the hypothesis that the CNS defects observed in *mmy* are not attributable exclusively to the lack of chitin.

These observations suggest that there are, most likely, some chitin-independent phenotypes associated with the *mmy* mutants. WGA staining is abolished in the tracheal cells of mature *mmy* embryos (Fig. 4K), but present in those of *kkv* mutants (Fig. 4N), suggesting that the absence of other products detectable by this lectin can be responsible for the more severe tracheal phenotype of *mmy* mutants when compared to *kkv* (Figs. 4J–O).

mmy cuticle and epidermis

Chitin is a component of the insect embryonic cuticle with a major role in its formation and assembly. The role of chitin in the *Drosophila* embryonic cuticle has recently been extensively analyzed (Moussian et al., 2005). In this study, it was shown that the embryonic cuticle of *kkv* embryos detaches from the body and looses its integrity but keeps some cuticular structures like the head skeleton, the denticle belts and the hairs. We analyzed cuticle preparations of *mmy* mutant embryos (Fig. 7B) and found that these cuticles are much more disrupted than those reported for *kkv* embryos (Moussian et al., 2005). No specific structures can be recognized, and there are no signs of denticle belts or hairs (Figs. 7B, B′); in some cases, we detected what could be remnants of the head skeleton and sclerotic fragments. Indeed, when *mmy* mutant embryos were devitelinized, we could not recover any cuticle preparation.

As in the trachea, both chitin and other GlcNAc containing products, as detected by WGA, were present in the wild-type embryonic cuticle but absent in *mmy* (Figs. 4A, B and 7C, D). However, while *kkv* embryonic cuticle lacks chitin, it still contains terminal GlcNAc residues as detected by WGA incorporation (Figs. 4C and 7E). Again, as in the tracheal system, this difference could explain the more dramatic effects on the embryonic cuticle of *mmy* embryos.

To examine in more detail the defects in *mmy* embryonic cuticle, we have also analyzed its structure by TEM. As described previously (Locke, 2001), in the wild-type cuticle of mature embryos, we could distinguish the envelope, the epicuticle and the procuticle; below these, an adhesion zone is thought to mediate the adhesion with the epidermal cells (Figs. 7F–G). Among these layers, the procuticle is composed of stacks of chitin laminae oriented parallel to one another in a highly organized structure (Fig. 7G). In *mmy* mature embryos, only the envelope and the epicuticle (Figs. 7H, I—arrowhead), the chitin-free layers, seem to maintain remainders of their structure. In particular, there is no sign of the highly organized structure of the procuticle, and the underlying epithelial cells appear detached in many places, indicating an overall disruption of the cuticle and its interaction with the epidermis (Fig. 7I—asterisk).

Discussion

In this work, we characterized new and previously described *mmy* and *cyst* mutations as mutant alleles of the CG9535 gene encoding UDP-GlcNAc diphosphorylase enzyme. This enzyme catalyzes the formation of UDP-GlcNAc, which is essential for chitin synthesis, membrane biosynthesis, protein N- and O-glycosylation and GPI anchor biosynthesis. This enzyme is well conserved and has clear homologues across different species. The human orthologue of the *Drosophila* gene is UAP1 which has been shown to be expressed in human sperm and to be the antigen responsible for antibody-mediated human infertility (Diekman and Goldberg, 1994). In *S. cerevisiae*, ScUAP1 deletions are lethal and mutants display an aberrant morphology (Mio et al., 1998, 1999). In the genome of *D. melanogaster*, Mummy is the only predicted UDP-GlcNAc diphosphorylase. Another enzyme involved in the UDP-GlcNAc metabolism is the UDP-GlcNAc epimerase that interconverts UDP-GlcNAc and UDP-GalNAc. This enzyme could provide an alternative route to UDP-GlcNAc synthesis and explain the relative mildness of the phenotypes in the absence of such a fundamental enzyme as UDP-GlcNAc diphosphorylase. However, there is no predicted UDP-GlcNAc epimerase in *D. melanogaster* (http://www.flybase.bio.indiana.edu; http://www.ebi.ac.uk). In view of the importance of UDP-GlcNAc diphosphorylase for the synthesis of UDP-GlcNAc and the ubiquitous requirement for this metabolite, we attribute the relatively mild phenotypes reported here and the survival of these embryos until later stages to the presence of a strong maternal contribution.

The embryonic phenotypes reported here for the *mmy* mutations arise as a consequence of the dwindling amounts of available UDP-GlcNAc. The production of different UDP-GlcNAc requiring molecules in different tissues is likely to exhibit variable sensitivity to the loss of UDP-GlcNAc diphosphorylase activity. The phenotypes observed may be due to the combined reduction of several UDP-GlcNAc containing products or primarily due to a lack of

Fig. 5. Expression of polarity, septate junction and fusion markers in *mmy* trachea, epidermis and salivary gland. (A–D) Wild-type and *mmy* dorsal trunks of stage 16 embryos stained for Sas, marking the apical side of the cells and GFP detecting the tauGFP construct present in all tracheal cells, highlighting their shape. Although the dorsal trunk of *mmy* mutants is severely affected, their cells have correctly placed apical surfaces facing the tracheal lumen. (E–H) Wild-type and *mmy* mutant dorsal trunk of stage 16 embryos stained for septate junction component (Dlg), Sas (apical marker) and anti-GFP; cell structure of mutant embryos is comparable to wild-type despite the visible tracheal defects. (I–L) Dlg co-localizes with Cora (another septate junction component), both in wild-type and *mmy* mutant trachea. Analysis of the *mmy* epidermis (O) and salivary gland (P) with the same septate junction components (Dlg and Cora) confirms that they are as correctly localized in other mutant *mmy* cells as in the wild-type (M, N). (Q–T) E-cadherin is correctly localized in *mmy* mutant tracheal cells, but the characteristic E-cadherin ring that marks the site of DT lumen fusion (arrow in Q) cannot be detected throughout the length of the *mmy* dorsal trunk. (U–X) The fusion3 reporter is expressed in both wild-type and *mummy*, highlighting the fusion cells (arrows in panels U and W) present in each segment of post-DT fusion stage 15 embryos. Panels A–L and U–X are confocal sections; panels M–T are confocal projections. epi = epidermis; sg = salivary gland.

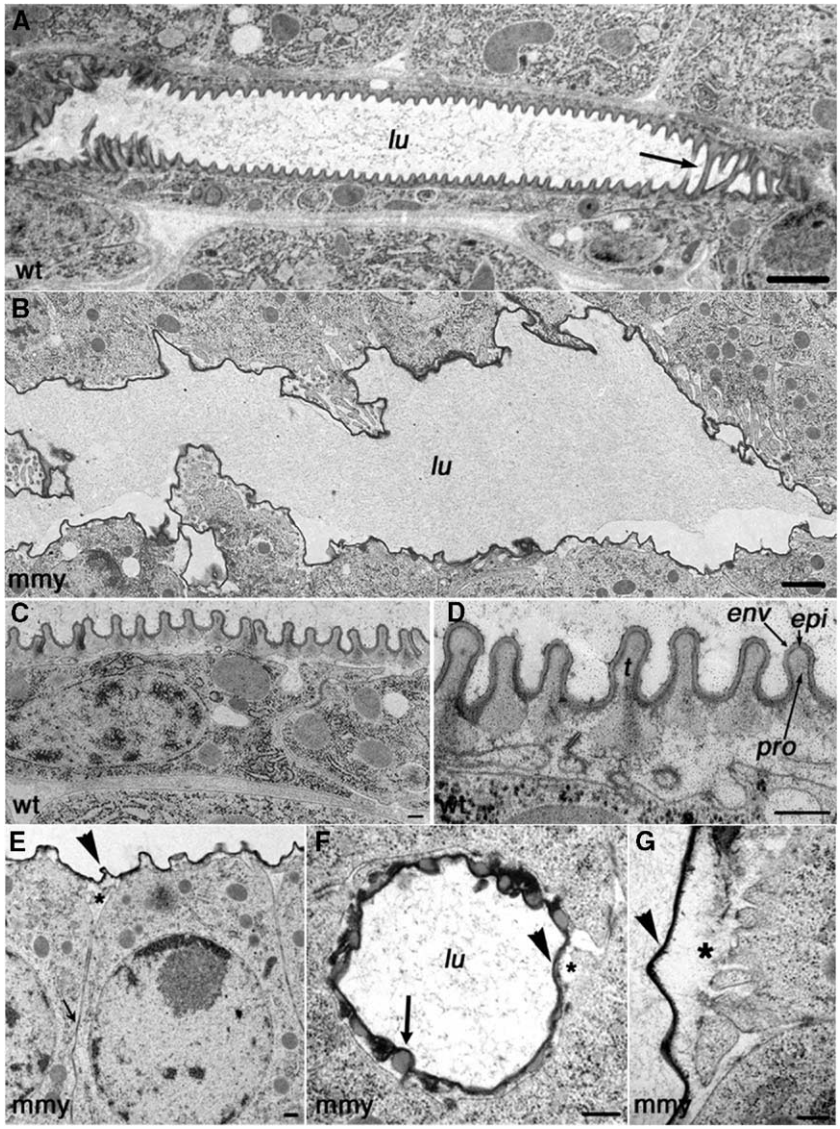

Fig. 6. Ultrastructure of the tracheal lumen of *mummy* mutants. Electron micrographs of wild-type and *mmy* homozygous embryos at the end of embryogenesis. Longitudinal sections of a wild-type (A) and *mmy* (B) dorsal trunk showing the lumenal structure and tracheal cells. The wild-type section is not at the middle of the dorsal trunk but at a more sagittal point, showing a tube that is not cut at its largest width; arrows (in A) point to the areas where the cut is most sagittal and the taenidial folds are seen closest to the luminal membrane, showing their characteristic ridges. (B) The *mmy* dorsal trunk section shows a highly disorganized structure with constrictions and dilations and no taenidial folds. (C and D) Detail of the wild-type structure of the taenidial folds in the dorsal trunk, showing the envelope, epicuticle and procuticle within each taenidium. (E–G) Detail of the luminal structure of *mmy* mutants; the luminal envelope is still formed (arrowheads in panels E, F and G), but there are no detectable taenidial folds. The cells that form the dorsal trunk in *mmy* mutants are the correct shape, and cell–cell junctions can be detected between them (arrow in E points at the septate junctions). In transversal cuts of the lateral trunk in *mmy* mutants, some electron dense structures can be detected (arrow in panel F), but no taenidial folds are formed. Mutant tracheal lumen shows a detachment between the cell membranes and the envelope and the microvillae that are involved in the formation of the lumenal cuticle can still be detected in the mutant even at this late stage (asterisk in panels B, E, F and G). Scale bars = 1 μm in panels A and B and = 200 nm in all others; env = envelope; epi = epicuticle; pro = procuticle; t = taenidium; lu = lumen.

one particular molecule. Here, we show that the tracheal and cuticle phenotypes are principally due to the lack of chitin. This absence of chitin is not responsible for the CNS phenotype present in *mmy* embryos as this defect is not present in mutants for the chitin synthase CS-1 (Ostrowski et al., 2002; Moussian et al., 2005). The CNS phenotype is likely to be due to a deficit in the appropriate glycosylation of one or more molecules. Normal development of the nervous system requires cellular interactions such as recognition and adhesion as well as the ability to send and receive signals. Many of these signaling interactions are mediated by glycoproteins, glycolipids and proteoglycans and GPI-linked proteins all of which would be affected by the reduction or absence of UDP-GlcNAc. The fidelity of axon fasciculation is known to be affected by alterations to glycan expression (Song and Zipser, 1995; Stoeckli and Landmesser, 1995), and carbohydrate binding proteins are required for accurate CNS development (Sharrow and Tiemeyer, 2001; Tang et al., 1994). GlcNAc is also a major constituent of the glycosaminoglycans which are added to heparan sulfate proteoglycans (HSPGs) which are required for multiple signaling path-

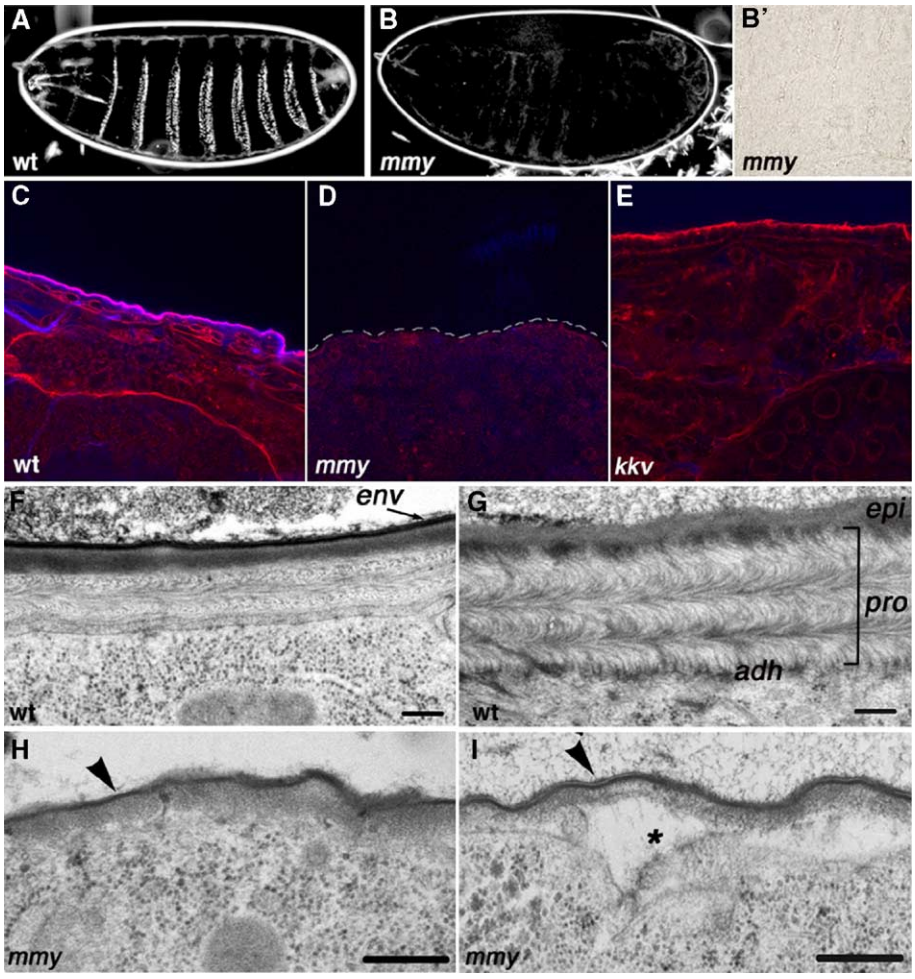

Fig. 7. Mutations in *mmy* affect cuticle morphology. The cuticle is absent from *mmy* embryos. (A, B) Dark field microscopy of cuticle preparations of mature wild-type and homozygous mutant *mmy* embryos. *mmy* mutant embryos do not form any detectable cuticle nor display any denticles. (B′) Bright field 40× magnification of panel B, confirming the absence of denticles in *mummy* embryos. (C–E) Confocal sections of wild-type, *mmy* and *kkv* embryonic epidermis stained with Fluostain (blue) and WGA (red). In wild-type embryos, we detect the presence of both chitin (blue) and *N*-acetylglucosamine (red) in the embryonic epidermis; in *mmy* mutant embryos, neither is detected (the limit of the epidermis is marked by a dashed white line) and in *kkv* mutants only chitin is absent. (F–I) Transmission electron microscope photographs of wild-type and *mmy* mature embryos. (F, G) In earlier wild-type embryos, the procuticle is not as broad, and the cuticular envelope is more electron dense (arrow in panel F). The envelope is a cuticular layer rich in protein that has been reported not to contain any chitin (Locke, 2001). In the procuticle of mature wild-type embryos, the chitin laminae are arranged in the typical helicoidal pattern, (G) and the epicuticle, procuticle and adhesion zones are clearly detected. (H, I) In *mmy* mutant embryos, the chitin-rich procuticle is never detected; in these embryos, the envelope is formed above a region that resembles the wild-type epicuticle (arrowheads in panels H, I); in older embryos, a detachment between the apical membrane of the epidermal cells and the envelope can be detected (asterisk in panel I). Scale bars = 200 nm; env = envelope; epi = epicuticle; pro = procuticle; adh = adhesion zone; arrowheads point at the cuticular envelope.

ways (Kramer and Yost, 2003; Yamaguchi, 2001). Recently, it has been demonstrated that the activity of Slit, a key midline derived signaling molecule that directs axon extension both across the midline and fascicle choice by longitudinal axons in *Drosophila*, is modulated by the HSPGs, Syndecan and Dallylike (Steigemann et al., 2004; Johnson et al., 2004) and that axon sorting in Zebrafish requires HSPG synthesis (Lee et al., 2004). Additionally, it has been suggested that an appropriate pattern of HSPGs is necessary for axons to select their appropriate pathways (Johnson et al., 2004). Here, we find that loss of UDP-GlcNAc diphosphorylase activity affects axon pathway choice, future work utilizing genetic interactions should identify which products become depleted to give rise to this CNS phenotype.

The tracheal mmy phenotype

The tracheal system of *mmy* mutant embryos appears to develop normally until the stage of tube formation. Even at later stages when these embryos are severely disrupted, the overall organization of the tracheal cells appears normal, at least in terms of their apical basal polarity and the restricted expression of the other proteins analyzed. Yet, at the same later stages, the general arrangement of the tracheal lumen is severely distorted. Noticeably, in mature *mmy* embryos, the luminal envelope is detached from the tracheal cell membrane. This emphasizes the fact that the proper tubular structure and its interaction with the surrounding cells can play an important role in maintaining the general constitution of the tracheal system following tube formation.

Secretion of luminal components is an important step during tube formation and expansion (Lubarsky and Krasnow, 2003). Vesicle-like structures have been reported to be involved both in tube expansion and in cuticle formation at the epidermis. During cuticle formation, microvillae are detected at the epidermal cell membranes prior to the formation of the cuticular envelope, and chitin is believed to be delivered to the cell surface via vesicles that fuse with the plasma membrane (Locke, 2001; Merzendorfer and Zimoch, 2003). In *mmy* mutants, as in *kkv*, we detected only the chitin-free envelope and the epicuticle because the chitin-rich procuticle is never synthesized. Failure to deliver chitin to the cell surface and the subsequent lack of the procuticle both in the trachea and in the epidermis result in the detachment of cells from the chitin-free cuticular structures, thereby affecting luminal and cuticle stability.

This contribution of the lack of chitin to the *mmy* phenotype is confirmed by the comparative analysis with *kkv* mutants. However, the *kkv* phenotypes constitute only a subset of those displayed by *mmy*. Detailed examination of *kkv* mutants indicates chitin-independent defects in the *mmy* tracheal system, particularly in what relates to the lack of lumen continuity of the dorsal trunk. In addition, the zygotic expression of *mmy* begins earlier (at stage 11) than *kkv* (at stage 13) (Moussian et al., 2005), long before chitin is synthesized in the tracheal lumen.

An additional lack of GlcNAc containing proteins at the cell surface or within the extracellular matrix could further affect the luminal stability in *mmy* embryos. In wild-type, at the site of fusion, after the fusion cells from adjacent metameres have made contact and the cadherin rings form, a lumen is formed inside at the junction between these cells. This lumen further expands to give rise to a continuous tube, and the tripartite cadherin remains at the site of fusion (Tanaka-Matakatsu et al., 1996). In *mmy* embryos, the fusion cells seem to be properly determined and to express adequate fusion markers, but a continuous lumen is rarely achieved. The observed defects could be due to structural problems aggravated by the absence of GlcNAc either in the tracheal lumen or in the structure of the cadherin ring itself. Additionally, as in the CNS, *mmy* tracheal defects not present in *kkv* could partly arise as a consequence of the impairment of a signaling process mediated by GlcNAc containing proteins. GlcNAc is a major component of glucosaminoglycan chains attached to heparan sulfate proteoglycans (HSPGs) that play a major role in multiple signaling pathways involving Wingless, Hedgehog, FGF or Decapentaplegic (reviewed in Lin, 2004; Blair, 2005).

A remarkable feature of the dorsal trunk of *mmy* embryos is the absence of taenidial folds, the annular rings around the tracheal lumen. As these structures are thought to provide some stiffness to the tracheal tubes, their absence could have an important influence in the irregular diameter of the dorsal trunk. Considering that during these developmental stages the tracheal lumen is filled with liquid (reviewed in Manning and Krasnow, 1993), regions of prominent expansions could reflect the lack of rigidity of the tubes. In combination with the failure to establish proper lumen continuity at the fusion points, lack of rigidity could be an important factor contributing to the overall bubble-like structure of *mmy* dorsal trunks. Finally, as described above, accumulation of Pio luminal protein seems to be unaffected in *mmy* mutants, as opposed to the accumulation of the lumen epitope recognized by the 2A12 antibody, suggesting that not all the luminal components are impaired in *mmy* mutants and that different luminal structures appear to be specified independently.

Specific genes for tube size? Mechanisms of tube size control in the Drosophila trachea

Different branches of the tracheal system have specific and distinct diameters and lengths. These features are very stereotyped and have been suggested to be under the control of a genetic program. Indeed, many genes have been unveiled that, when mutated, produce enlargements or expansions of the tubes (Beitel and Krasnow, 2000). Some of these genes have been recently characterized and, despite being originally identified as controlling tube length, have been found to code for proteins belonging or associated to the septate junctions (SJs). However, besides their effect on tube length, mutations on these genes also cause a failure in the trans-epithelial diffusion barrier (Behr et al., 2003; Hemphala et al., 2003; Paul et al., 2003; Llimargas et al., 2004; Wu et al., 2004). Among the genes influencing tube size, *cyst*/*mmy* has been singled out as a diameter-specific regulatory gene (Beitel and Krasnow, 2000; Wu and Beitel, 2004). Here, we show that the tracheal tube expansions, constrictions and consequent diameter variations in *mmy* mutants reflect a severe disorganization of lumen structure. In fact, many of the tracheal branches of the *mmy* mutants have lost their tubular characteristic and form collapsed independent vesicle-like structures. Thus, besides affecting tube diameter, the *mmy* gene is involved in the proper organization of the tracheal cells and tracheal luminal cuticle, and the expansions and constrictions seem to be side effects of disrupting these events.

The above-mentioned observations suggest that many of the genes that have been ascribed to the genetic control of tube size may simply be required for cell arrangement, proper tube fusion and/or physiological and cuticle organization of the tracheal tube epithelia. In this regard, *mmy*, *kkv* and even the SJ mutants do not appear to modify just the tube size itself, but also its organization, bringing into doubt whether there is a specific genetic size-control program. Conversely, we would like to suggest that many features of tube size might not be under the independent control of a specific genetic program but, instead, that size may be a structural property of the organization of each specific branch. According to this view, the size control of a particular tube would not be something imposed upon a branch but rather a consequence of its cellular organization. For example, while in some branches the surfaces of two or more cells contribute to the luminal circumference ("multicellular tubules"), in most branches, the tube circumference is made from single cells wrapped around the lumen ("unicellular tubules") (Jazwinska et al., 2003). Consistently, "multicellular tubules" are wider than "unicellular tubules,"

and it has been recently shown that the latter are originated by cell intercalation, a process that it is under genetic control (Jazwinska et al., 2003; Ribeiro et al., 2004). Thus, tube diameter could be indirectly controlled by the program regulating cell intercalation. Similarly, tracheal cell shapes are very different in the branches formed along the anteroposterior axis compared to the ones formed along the dorsoventral axis; the former ones adopt an elongated shape, while the latter remain cuboidal (Llimargas and Casanova, 1999). As these cell shapes are also related to the basic organization of the different tracheal branches, they could also contribute to the final length of the tubes. Again, this difference in cell shape is regulated by the specific signaling pathways responsible for the migration in one or the other axis. Thus, once the basic organization of the distinct branches is set, the remaining process of lumen formation and the final thickness of the tracheal epithelium could be a determinant for the final size of the tubes.

Finally, the basic features of the specific branches are also determined by the constraints of the surrounding tissues. First, the dynamic expression of the branchless (Bnl) chemoattractant molecule will determine the final position acquired by the tracheal branches (Sutherland et al., 1996). And, second, the topological constraints will also have a role in the process. Thus, for instance, development of the dorsal trunk requires the existence of a population of lateral mesoderm cells that act as a substrate for migration of the tracheal cells forming this branch, whereas formation of the dorsal branch requires tracheal cell migration through a groove of muscle precursor cells of defined width (Franch-Marro and Casanova, 2000). In summary, we would like to suggest that many features of tube size are not under the independent control of a specific genetic program but instead are derived from both the surrounding constraints and the distinct organization properties of each particular branch.

Materials and methods

Drosophila strains

The mutants used in this study are: mmy^{H053}, mmy^{GA74}, mmy^{GA760} (from EMS mutagenesis), mmy^{cys} (Beitel and Krasnow, 2000) and kkv^{14C73} (Moussian et al., 2005). Deficiencies and other *Drosophila* strains are from the Bloomington *Drosophila* Stock Center. To identify homozygous mutant embryos, we used the second or third chromosome carrying blue or GFP balancers: CyO-*wg*-lacZ, CyO-Kr-GFP and TM3-*twi*-GFP. The wild-type strain utilized was *yw*. *Drosophila* stocks and crosses were kept on standard conditions at 25°C.

Immunostaining, in situ hybridization and permeabilization assays

Embryos were staged according to Campos-Ortega and Hartenstein (1985) and stained according to standard protocols. Immunostaining was performed on embryos fixed in 4% formaldehyde for 10–30 min, except for anti-Pio staining, for which we fixed using 11% formaldehyde (Jazwinska et al., 2003). The following antibodies were used: anti-GFP (Molecular Probes), anti-E-cad, mAb2A12, mBP102 and m1D4 (Developmental Studies Hybridoma Bank-DSHB), anti-Trh (our own stock, made by N. Martín), anti-Sas (from D. R. Cavener), anti-Dlg (from A. Müller), anti-Cora (from R. G. Fehon), anti-Pio (from M. Affolter) and anti-βGal (Cappel). Biotinylated or Cy3, FITC and Cy5 secondary antibodies (Jackson ImmunoResearch) were used at a dilution of 1/500. For HRP histochemistry, the signal was amplified using the Vectastain–ABC kit (Vector Laboratories) when required. For fluorescent staining, the signal was amplified using TSA (NEN Life Sciences) when required. Chitin was visualized by the fluorescence of incorporated Fluostain (Sigma) at 1 μg/ml. The wheat germ agglutinin conjugates used were WGA-Tetramethylrhodamine and WGA-Alexa Fluor® 633 (Molecular Probes) at 4 μg/ml. Embryos were fixed as standard and then incubated with Fluostain and/or WGA diluted in PBST for 2–4 h at room temperature or overnight at 4°C. Photographs were taken using Nomarski optics or fluorescence in a Nikon Eclipse 80i microscope. Confocal images were obtained with a Leica TCS-SP2-AOBS system, Leica DM IRE2 microscope and LCS software. Permeabilization assays were performed by injecting rhodamine-labeled dextran (*M*r 10,000; Molecular Probes) into the body cavity of embryos, as described (Lamb et al., 1998). In situ hybridization was performed according to standard protocols, with *mmy* RNA probes generated using the whole cDNA as template and produced using the Megascript kit (Ambion).

Molecular analysis

Genomic DNA isolation, PCR amplification and sequencing were performed according to standard techniques. For the identification of the mutations in the *mmy* alleles studied, the *mmy* genomic region (CG9535) was amplified by PCR from homozygous mutant embryos and sequenced using specific primers. MacVector (Accelrys) was used for DNA and protein sequence analysis.

Electron microscopy

Wild-type or homozygous mutant *Drosophila* late stage 16–17 embryos were selected under a stereomicroscope and transferred to 1.5 mm diameter and 200 μm depth planchettes filled with yeast paste (McDonald and Müller-Reichert, 2002; Müller-Reichert et al., 2003) and immediately cryoimmobilized using a Leica EMPact high-pressure freezer (Leica, Vienna, Austria) and then stored in liquid nitrogen until further use. They were freeze-substituted over 3 days at −90°C in anhydrous acetone containing 2% osmium tetroxide and 0.1% uranyl acetate at −90°C for 72 h and warmed to room temperature, 5°C per hour (EM AFS, Leica, Vienna, Austria). After several acetone rinses, samples were infiltrated with Epon resin during 2 days and polymerized at 60°C during 48 h. Ultrathin sections were obtained using a Leica Ultracut UCT ultramicrotome and mounting on Formvar-coated copper grids. They were stained with 2% uranyl acetate in water and lead citrate. Then, sections were observed in a JEM-1010 electron microscope (Jeol, Japan), and photographic negatives were scanned (Artixcan 2500f Microtek).

Note added in proof

A new paper has just been published reporting the involvement of chitin synthase in tracheal development (Tonning et al., 2005). It proposes an earlier role for chitin during tracheal development which does not alter our discussion on the link between tube morphogenesis and the regulation of tube size control.

Acknowledgments

We thank Carmen López-Iglesias and her group from the Serveis Cientificotècnics of the Universitat de Barcelona for the excellent electron microscopy work; Lídia Bardia for the confocal microscopy technical support and advice; Greg Beitel and the Bloomington Stock Center for providing some of the flies used in this study; and Samantha Alsbury for contributing to the molecular characterization. We are grateful to all

members of the Casanova and Tear laboratories for the continuous support and discussions. We thank Véronique Brodu, Marta Llimargas, Rui Martinho, Marco Milán and Daniel Shaye for critically reading the manuscript. S.J.A. acknowledges an I3P postdoctoral contract from the Consejo Superior de Investigaciones Cientificas (CSIC). S.J.A. and J.C. were funded by the CIRIT of the Generalitat de Catalunya and the Ministerio de Ciencia y Tecnología de España; H.A. and G.T. were funded by the Medical Research Council (MRC).

References

Araújo, S.J., Tear, G., 2003. Axon guidance mechanisms and molecules: lessons from invertebrates. Nat. Rev., Neurosci. 4, 910–922.

Behr, M., Riedel, D., Schuh, R., 2003. The claudin-like megatrachea is essential in septate junctions for the epithelial barrier function in *Drosophila*. Dev. Cell 5, 611–620.

Beitel, G.J., Krasnow, M.A., 2000. Genetic control of epithelial tube size in the *Drosophila* tracheal system. Development 127, 3271–3282.

Blair, S.S., 2005. Cell signaling: wingless and glypicans together again. Curr. Biol. 15, 92–94.

Boube, M., Martín-Bermudo, M.D., Brown, N.H., Casanova, J., 2001. Specific tracheal migration is mediated by complementary expression of cell surface proteins. Genes Dev. 15, 1554–1562.

Bulik, D.A., van Ophem, P., Manning, J.M., Shen, Z., Newburg, D.S., Jarroll, E.L., 2000. UDP-*N*-acetylglucosamine pyrophosphorylase, a key enzyme in encysting Giardia, is alosterically regulated. J. Biol. Chem. 275, 14722–14728.

Campos-Ortega, A.J., Hartenstein, V., 1985. The Embryonic Development of Drosophila Melanogaster. Springer-Verlag, New York, pp. 10–84.

Chihara, T., Hayashi, S., 2000. Control of tracheal tubulogenesis by Wingless signaling. Development 127, 4433–4442.

Diekman, A.B., Goldberg, E., 1994. Characterization of a human antigen with sera from infertile patients. Biol. Reprod. 50, 1087–1093.

Fehon, R.G., Dawson, I.A., Artavanis-Tsakonas, S., 1994. A *Drosophila* homologue of membrane-skeleton protein 4.1 is associated with septate junctions and is encoded by the coracle gene. Development 120, 545–557.

Franch-Marro, X., Casanova, J., 2000. The alternative migratory pathways of the *Drosophila* tracheal cells are associated with distinct subsets of mesodermal cells. Dev. Biol. 270, 80–90.

Hemphala, J., Uv, A., Cantera, R., Bray, S., Samakovlis, C., 2003. Grainy head controls apical membrane growth and tube elongation in response to Branchless/FGF signalling. Development 130, 249–258.

Herscovics, A., Orlean, P., 1993. Glycoprotein biosynthesis in yeast. FASEB J. 7, 540–550.

Ikeya, T., Hayashi, S., 1999. Interplay of Notch and FGF signaling restricts cell fate and MAPK activation in the *Drosophila* trachea. Development 126, 4455–4463.

Jazwinska, A., Ribeiro, C., Affolter, M., 2003. Epithelial tube morphogenesis during *Drosophila* tracheal development requires Piopio, a luminal ZP protein. Nat. Cell Biol. 5, 895–901.

Johnson, K.G., Ghose, A., Epstein, E., Lincecum, J., O'Connor, M.B., Van Vactor, D., 2004. Axonal heparan sulfate proteoglycans regulate the distribution and efficiency of the repellent slit during midline axon guidance. Curr. Biol. 14, 499–504.

Kramer, K.L., Yost, H.J., 2003. Heparan sulfate core proteins in cell–cell signaling. Annu. Rev. Genet. 37, 461–484.

Lamb, R.S., Ward, R.E., Schweizer, L., Fehon, R.G., 1998. Drosophila coracle, a member of the protein 4.1 superfamily, has essential structural functions in the septate junctions and developmental functions in embryonic and adult epithelial cells. Mol. Biol. Cell 9, 3505–3519.

Lee, S., Kolodziej, P.A., 2002. The plakin Short Stop and the RhoA GTPase are required for E-cadherin dependent apical surface remodeling during tracheal tube fusion. Development 129, 1509–1520.

Lee, J.S., von der Hardt, S., Rusch, M.A., Stringer, S.E., Stickney, H.L., Talbot, W.S., Geisler, R., Nusslein-Volhard, C., Selleck, S.B., Chien, C.B., Roehl, H., 2004. Axon sorting in the optic tract requires HSPG synthesis by ext2 (dackel) and extl3 (boxer). Neuron 44, 947–960.

Lin, X., 2004. Functions of heparan sulfate proteoglycans in cell signaling during development. Development 131, 6009–6021.

Llimargas, M., 1999. The Notch pathway helps to pattern the tips of the *Drosophila* tracheal branches by selecting cell fates. Development 126, 2355–2364.

Llimargas, M., 2000. Wingless and its signalling pathway have common and separable functions during tracheal development. Development 127, 4407–4417.

Llimargas, M., Casanova, J., 1997. *ventral veinless*, a POU domain transcription factor, regulates different transduction pathways required for tracheal branching in *Drosophila*. Development 124, 3273–3281.

Llimargas, M., Casanova, J., 1999. EGF signalling regulates cell invagination as well as cell migration during formation of tracheal system in *Drosophila*. Dev. Genes Evol. 209, 174–179.

Llimargas, M., Strigini, M., Katidou, M., Karagogeos, D., Casanova, J., 2004. Lachesin is a component of a septate junction based mechanism that controls tube size and epithelial integrity in the *Drosophila* tracheal system. Development 131, 181–190.

Locke, M., 2001. The Wigglesworth lecture: insects for studying fundamental problems in biology. J. Insect Physiol. 47, 495–507.

Lubarsky, B., Krasnow, M.A., 2003. Tube morphogenesis: making and shaping biological tubes. Cell 112, 19–28.

Manning, G., Krasnow, M.A., 1993. Development of the *Drosophila* tracheal system. In: Bate, M., Martínez-Arias, A. (Eds.), The Development of *Drosophila melanogaster*. Cold Spring Harbor Laboratory Press, Cold Spring Harbor, NY, pp. 609–685.

McDonald, K., Müller-Reichert, T., 2002. Cryomethods for thin section electron microscopy. Methods Enzymol. 351, 96–123.

Merzendorfer, H., Zimoch, L., 2003. Chitin metabolism in insects: structure, function and regulation of chitin synthases and chitinases. J. Exp. Biol. 206, 4393–4412.

Mio, T., Yabe, T., Arisawa, M., Yamada-Okabe, H., 1998. The eukaryotic UDP-*N*-acetylglucosamine pyrophosphorylases. Gene cloning, protein expression, and catalytic mechanism. J. Biol. Chem. 273, 14392–14397.

Mio, T., Yamada-Okabe, T., Arisawa, M., Yamada-Okabe, H., 1999. *Saccharomyces cerevisiae* GNA1, an essential gene encoding a novel acetyltransferase involved in UDP-*N*-acetylglucosamine synthesis. J. Biol. Chem. 274, 424–429.

Moussian, B., Schwarz, H., Bartoszewski, S., Nüsslein-Volhard, C., 2005. Involvement of chitin in exoskeleton morphogenesis in *Drosophila melanogaster*. J. Morphol. 264, 117–130.

Müller-Reichert, T., Hohenberg, H., O'Toole, E.T., McDonald, K., 2003. Cryoimmobilization and three-dimensional visualization of *C. elegans* ultrastructure. J. Microsc. 212, 71–80.

Nüsslein-Volhard, C., Wieschaus, E., Kluding, H., 1984. Mutations affecting the pattern of the larval cuticle in *Drosophila melanogaster*: I. Zygotic loci on the second chromosome. Wilhelm Roux's Arch. Dev. Biol. 193, 267–282.

Ostrowski, S., Dierick, H.A., Bejsovec, A., 2002. Genetic control of cuticle formation during embryonic development of *Drosophila melanogaster*. Genetics 161, 171–182.

Paul, S.M., Ternet, M., Salvaterra, P.M., Beitel, G.J., 2003. The Na/K ATPase is required for septate junction function and epithelial tube-size control in the *Drosophila* tracheal system. Development 130, 4963–4974.

Peneff, C., Mengin-Lecreulx, D., Bourne, Y., 2001. The crystal structures of Apo and complexed *Saccharomyces cerevisiae* GNA1 shed light on the catalytic mechanism of an amino-sugar *N*-acetyltransferase. J. Biol. Chem. 276, 16328–16334.

Ribeiro, C.M., Neumann, M., Affolter, M., 2004. Genetic control of cell intercalation during tracheal morphogenesis in *Drosophila*. Curr. Biol. 14, 2197–2207.

Samakovlis, C., Hacohen, N., Manning, G., Sutherland, D.C., Guillemin, K., Krasnow, M., 1996a. Development of the *Drosophila* tracheal system

occurs by a series of morphologically distinct but genetically coupled branching events. Development 122, 1395–1407.

Samakovlis, C., Manning, G., Steneberg, P., Hacohen, N., Cantera, R., Krasnow, M.A., 1996b. Genetic control of epithelial tube fusion during *Drosophila* tracheal development. Development 122, 3531–3536.

Schonbaum, C.P., Organ, E.L., Qu, S., Cavener, D.R., 1992. The *Drosophila melanogaster* stranded at second (sas) gene encodes a putative epidermal cell surface receptor required for larval development. Dev. Biol. 151 (2), 431–445.

Sharrow, M., Tiemeyer, M., 2001. Gliolectin-mediated carbohydrate binding at the *Drosophila* midline ensures the fidelity of axon pathfinding. Development 128, 4585–4595.

Song, J., Zipser, B., 1995. Targeting of neuronal subsets mediated by their sequentially expressed carbohydrate markers. Neuron 14, 537–547.

Steigemann, P., Molitor, A., Fellert, S., Jackle, H., Vorbruggen, G., 2004. Heparan sulfate proteoglycan syndecan promotes axonal and myotube guidance by slit/robo signaling. Curr. Biol. 14, 225–230.

Steneberg, P., Englund, C., Kronhamm, J., Weaver, T.A., Samakovlis, C., 1998. Translational readthrough in the hdc mRNA generates a novel branching inhibitor in the *Drosophila* trachea. Genes Dev., 956–967.

Steneberg, P., Hemphala, J., Samakovlis, C., 1999. Dpp and Notch specify the fusion cell fate in the dorsal branches of the *Drosophila* trachea. Mech. Dev. 87, 153–163.

Stoeckli, E.T., Landmesser, L.T., 1995. Axonin-1, Nr-CAM, and Ng-CAM play different roles in the in vivo guidance of chick commissural neurons. Neuron 6, 1165–1179.

Sutherland, D., Samakovlis, C., Krasnow, M.A., 1996. *Branchless* encodes a *Drosophila* FGF homolog that controls tracheal cell migration and the pattern of branching. Cell 87, 1091–1101.

Tanaka-Matakatsu, M., Uemura, T., Oda, H., Takeichi, M., Hayashi, S., 1996. Cadherin-mediated cell adhesion and cell motility in *Drosophila* trachea regulated by the transcription factor escargot. Development 122, 3697–3705.

Tang, J., Rutishauser, U., Landmesser, L., 1994. Polysialic acid regulates growth cone behavior during sorting of motor axons in the plexus region. Neuron 13, 405–414.

Tonning, A., Hemphälä, J., Tång, E., Nannmark, U., Samakovlis, C., Uv, A., 2005. A transient luminal chitinous matrix is required to model epithelial tube diameter in the *Drosophila* trachea. Dev. Cell 9 (3), 423–430.

Vincent, S., Ruberte, E., Grieder, N.C., Chen, C., Haerry, T., Schuh, R., Affolter, M., 1997. DPP controls tracheal cell migration along the dorsoventral body axis of the *Drosophila* embryo. Development 124, 2741–2750.

Wappner, P., Gabay, L., Shilo, B.-Z., 1997. Interactions between the EGF receptor and DPP pathways establish distinct cell fates in the tracheal placodes. Development 124, 4707–4716.

Woods, D.F., Bryant, P.J., 1991. The discs-large tumor suppressor gene of *Drosophila* encodes a guanylate kinase homolog localized at septate junctions. Cell 66, 451–464.

Wright, C.S., 1984. Structural comparison of the two distinct sugar binding sites in wheat germ agglutinin isolectin II. J. Mol. Biol. 178, 91–104.

Wu, V.M., Beitel, G.J., 2004. A junctional problem of apical proportions: epithelial tube-size control by septate junctions in the *Drosophila* tracheal system. Curr. Opin. Cell Biol. 16, 493–499.

Wu, V.M., Schulte, J., Hirschi, A., Tepass, U., Beitel, G.J., 2004. Sinuous is a *Drosophila* claudin required for junction organization and epithelial tube size. J. Cell Biol. 164, 313–323.

Yamaguchi, Y., 2001. Heparan sulfate proteoglycans in the nervous system: their diverse roles in neurogenesis, axon guidance, and synaptogenesis. Semin. Cell Dev. Biol. 12, 99–106.